Physica A 191 (1992) 263–276
North-Holland

PHYSICA A

Simulation of granular media

H.J. Herrmann
Höchstleistungsrechenzentrum, KFA, W-5170 Jülich, Germany

The flow of granular material, like sand, presents many intriguing effects in particular when it is shaken, poured or sheared. Here, the granular medium is modelled by a packing of elastic spheres and simulated via molecular dynamics. Dissipation of energy and shear friction at collisions are included. The onset of fluidization can be determined and is in good agreement with experiments. On a vibrating plate we observe the formation of convection cells due to walls or amplitude modulations. Density and velocity profiles on conveyor belts are measured and the influence of an obstacle discussed. We mention various types of rheology for flow down an inclined chute or through a pipe and outflowing containers. We also briefly sketch a thermodynamic formalism for granular material.

One encounters a rich variety of astonishing, scarcely understood phenomena when granular materials like sand or powder move [1,2]. Examples are the so-called "Brazil nut" segregation [3–5], heap formation under vibration [6–8], density waves emitted from outlets [9] and $1/f$ noise in the power spectra of local forces [10]. All these effects seem to eventually originate in the ability of granular materials to form a hybrid state between a fluid and a solid: When the density exceeds a certain value, the critical dilatancy [11,12], it is resistant to shear, like solids, while below this density it will "fluidify". This fluidified state can be rather complex, specially in the presence of density fluctuations and density gradients.

In order to formalize and quantify the complicated rheology of granular media various attempts have been made. Continuum equations of motion [13], a cellular automaton [14] and a random walk approach [15] have been proposed. But most of the above mentioned effects have so far not been satisfactorily explained by these techniques. This is because much basic understanding of the relevant mechanisms is still lacking – even for the concept of fluidization various definitions are possible [16].

Particularly suited to study this fluidization is an experiment where sand is put on a loudspeaker or on a vibrating table [6–8,17,18]. Under gravity the sand jumps up and down and although kinetic energy is strongly dissipated, collisions among the grains reduce its density thereby allowing it to flow ("fluidization"). Under certain circumstances flow between top and bottom can

occur in the form of convection cells as has been observed experimentally in the case of inhomogeneities in the amplitude of the vibration [19]. Also within the heaps [6–8] convection occurs and might even be the motor for the heap formation. When the vibration of the plate also has a horizontal component the material will flow in one direction, a technique often used in powder transport.

I will discuss in the following molecular dynamics (MD) simulations of inelastic particles with an additional shear friction in two dimensional systems performed with J. Gallas and S. Sokolowski. We present data for the onset of fluidization [16] and give evidence for the occurrence of convection cells due to inhomogeneities in the vibration amplitude or due to walls, an effect that has also been observed recently [20,21]. We also report on measurements of the velocity and density profiles of powder transported on a vibrating belt [22]. In fact, MD simulations [23,24] have already been applied to granular media to model segregation [5], outflow from a hopper [25,26], shear flow [27] and flow down an inclined chute [28].

We consider a system of N spherical particles of equal density and with diameters d chosen randomly from a homogeneous distribution of width w around $d_0 = 1$ mm. These particles are placed into a container of width L that is open on the top and has either periodic boundary conditions or fixed walls in the horizontal direction. When two particles i and j overlap (i.e. when their distance is smaller than the sum of their radia) three forces act on particle i: (i) an elastic restoration force,

$$f_{\mathrm{el}}^{(i)} = Ym_i[|\boldsymbol{r}_{ij}| - \tfrac{1}{2}(d_i + d_j)] \frac{\boldsymbol{r}_{ij}}{|\boldsymbol{r}_{ij}|} , \tag{1a}$$

where Y is the Young modulus (normalized by the mass), $m_i \propto d_i^2$ the mass of particle i and $\boldsymbol{r}_{ij}$ points from particle i to j; (ii) a dissipation due to the inelasticity of the collision,

$$f_{\mathrm{diss}}^{(i)} = -\gamma m_i(\boldsymbol{v}_{ij} \cdot \boldsymbol{r}_{ij}) \frac{\boldsymbol{r}_{ij}}{|\boldsymbol{r}_{ij}|^2} , \tag{1b}$$

where γ is a phenomenological dissipation coefficient and $\boldsymbol{v}_{ij} = \boldsymbol{v}_i - \boldsymbol{v}_j$ the relative velocity; (iii) a shear friction force that mimics to some degree the effect of solid friction,

$$f_{\mathrm{shear}}^{(i)} = -\gamma_{\mathrm{s}} m_i(\boldsymbol{v}_{ij} \cdot \boldsymbol{t}_{ij}) \frac{\boldsymbol{t}_{ij}}{|\boldsymbol{r}_{ij}|^2} , \tag{1c}$$

where γ_{s} is the shear friction coefficient and $\boldsymbol{t}_{ij} = (-r_{ij}^y, r_{ij}^x)$ is the vector $\boldsymbol{r}_{ij}$ rotated by 90°. As compared to other modelizations of the forces acting

between grains [5,25,27,29,30] our equations (1) are simpler since we neglect Coulomb friction and the rotation of particles. In fact, solid friction should be proportional to the normal force but the term of eq. (1c) is always needed to halt the tangential relative motion [29]. We did these simplifications on purpose in order to have less, in our opinion unimportant, fit parameters. In fact, under realistic deviations from the spherical shape of the particles rotations are strongly suppressed.

When a particle collides with a wall the same forces act as if it would have encountered another particle of diameter d_0 at the collision point. Two forces act on the system, on one hand gravitation $g \approx -10\,\mathrm{m/s^2}$ pulls each particle down, on the other hand the bottom of the container is subjected to a vibrating motion described by

$$z_0(t) = A(x)\sin(2\pi f t)\,, \tag{2}$$

where f is the frequency and A the amplitude. In some applications we will consider an explicit spatial modulation of A of the form

$$A(x) = A_0[1 - B\cos(2\pi x/L)]\,. \tag{3}$$

For vibrating conveyor belts this plate undergoes harmonic oscillations in both horizontal (x) and vertical (z) directions according to

$$x(t) = A_x \sin(2\pi f t) \quad \text{and} \quad z(t) = A_z \sin(2\pi f t)\,, \tag{4}$$

where f is the frequency and A_x and A_z are x and z amplitudes, respectively. The corresponding angle of the composed oscillation is $\alpha = \arctan(A_z/A_x)$.

Two initial positions of the particles are considered: they are either placed regularly on the bottom of the container or put at random positions inside a space several times as high as the dense packing. The initial velocities are either zero or randomly chosen. After that the particles are allowed to fall freely under gravity and relax for a time that corresponds to ten or twenty cycles of the vibration. The displacements, velocities and energies are then measured by averaging over up to 200 cycles. We use a fifth order predictor–corrector MD with $(2\text{–}6) \times 10^3$ iteration steps per cycle which vectorizes on the Cray-YMP, running at about $10\,\mu\mathrm{s}$ per particle-update for $N = 200$.

A recent paper [17] reported experimental observations of a "fluidized" state in a 2D vertical packing of steel spheres submitted to vertical vibrations. They shake periodically (at $f = 20$ Hz) 300 steel beads inside a trapezoidal cell with side walls tilted by 30° with respect to the vertical axis. Positions and velocities of the particles were obtained by photographing the system periodically and

then averaging over 15 snapshots taken at a given constant phase φ. Velocities were obtained from averages over a time interval τ around the phase φ. From a plot of the density of particles they argued fluidization to occur in the upper region of the packing. They found a curious effect: the mean density was found not to depend on the phase of the vibration, implying the appearance of a steady state preserving the density profile at all times, independent of the up and down collective motion. We wanted to reproduce numerically the phenomena observed in ref. [17] and to quantify the concept of fluidization.

With J. Gallas and S. Sokolowski we did simulations [16] of precisely the same geometry and number of particles as in the experiment. Fig. 1 shows local densities along the z-axis, evaluated at different phases as described in the experimental paper: (a) is the experiment [17] and (b) our simulation. Our curves were obtained by averaging the local density over the 15 ms following each phase φ and over 30 shaking cycles after discarding 30 "transient" cycles. As can be seen from this figure, our model correctly reproduces the experimen-

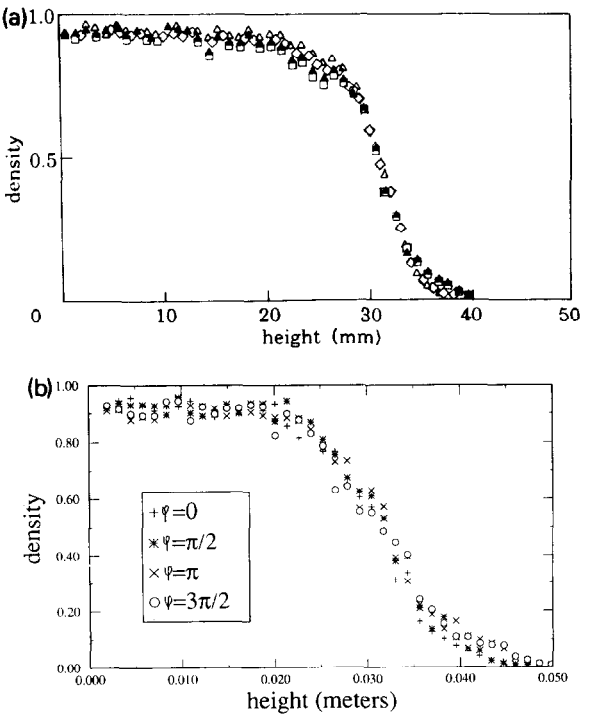

Fig. 1. Local density, normalized by the solid density, as a function of the height z for different phases of the vibration for $A = 2.5$, $f = 20$ Hz averaged over 30 shaking cycles after having discarded 30 cycles in order to reach steady state; (a) experiment of ref. [17] and (b) our simulation.

tal behaviour of the beads, producing the same smoothly varying density profile as function of the height z.

To check whether the present model is at all able to display a transition from a solid- to a fluid-like state we varied both frequency f and amplitude A of the oscillations. We recorded the trajectory of a selected "tracer" particle, and monitored its motion as time evolved. In the solid-like case the tracer particle remains confined to a very small region while in the fluid-like case the trajectory seems to explore the entire box. It is important to note that both situations can occur for the same value of Af^2 which means that Af^2 is not a good scaling variable even close to the onset of fluidization.

Let us next consider the case of a spatial modulation in the amplitude of the vibration, i.e. $B \neq 0$ in eq. (3), using periodic boundary conditions [20]. In fig. 2 we see the displacements of the particles after 15 cycles for $B = 0.5$. Clearly the particles flow upwards in the center where the amplitude of the vibrations is larger and form two convection cells. If the dissipation coefficient γ is increased by a factor of ten the convection is completely suppressed while it is quite insensitive to γ_s, even if $\gamma_s = 0$. The elastic modulus also has only a very weak influence as long as it remains larger than 10^3 (in units of d_0). The initial condition plays no noticeable effect showing that convection is no transient effect. The polydispersity w of the particles only slightly distorts the shape of the convection cells.

The strength of the convection was measured quantitatively by recording the average vertical components of the velocities of the particles in the center and at the edges. These quantities have also been measured experimentally by Rátkai [19]. The strongest convection for the aforementioned parameters is

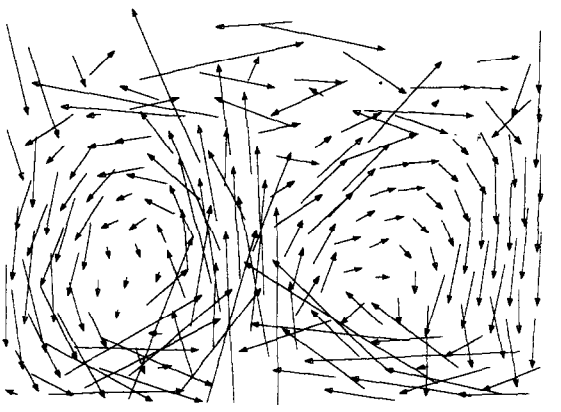

Fig. 2. Displacement of the particles after 15 cycles for $f = 70$ Hz using 200 particles in a box with periodic boundary conditions of size $L/d_0 = 20$ with $A_0 = 1.5d_0$, $B = 0.5$, $w = 0$, $Y = 5000/d_0$, $\gamma = 20g$, $\gamma_s = 200g/f$.

obtained around 60 Hz and it increases dramatically with the amplitude A_0 as was also seen in the experiment [19]. This resonance seems to be the driving force of the convective motion.

A completely different type of convection can be caused by the existence of fixed vertical walls without any modulation of the amplitude [20], i.e. for $B = 0$. One sees in fig. 3a for $\gamma_s = 0$ convection cells where the motion of the particles at the wall is upward. On the other hand, when $\gamma_s \neq 0$ there is at each wall a very strong downward drag giving rise to a convection in the opposite sense as seen in fig. 3b. The two convection cells remain attached to the walls showing that the walls are at the origin of these cells. One also recognizes a slight heap formation close to the wall, which might be a first sign of the famous sand heaps discovered by Faraday [6–8].

Let us analyse the origin of the convection due to fixed vertical walls. In the case of no shear friction the vertical walls do not transfer any vibrating motion of the container but represent only a steric hindrance to the flow. In this case, the following scenario applies: When, after levitating from the plate, the packing falls back on the bottom of the container only the horizontal component of the velocities of the particles arriving first will survive collisions with the downwards vertical motion of the rest of the packing that follows behind. So flow parallel to the bottom plate will spontaneously appear and is reinforced at each cycle. This parallel flow will only survive in regions where it is coherent and the size of these regions will grow due to the reinforcement. When one of these regions collides with a vertical wall the flow must go upwards since it cannot go anywhere else. This explains not only the orientation of the convection but also why the convection cells are attached to the walls as seen in fig. 3a. The driving force for these cells are therefore the horizontal flows along the bottom plate.

When shear friction with the wall is present a different mechanism sets in: While the particles are pushed up and start to levitate, the packing is still quite compressed and so a strong pressure is exerted on the walls giving rise to a strong shear friction while the relative motion of the particles with respect to the walls is upward. When afterwards the particles fall back and have downward relative motion with respect to the wall the packing is much looser and the shear friction much less efficient. Therefore the upward motion of the particles with respect to the wall is slowed down stronger, resulting in a net drag down along the wall. If γ_s is strong enough this effect can overcome the effect described in the above paragraph and the convection can reverse its orientation (fig. 3b.)

Let us next discuss the behaviour of vibrating conveyor belts [22], i.e. granular material under harmonic vibrations having a given angle with respect to the direction of gravity as described in eq. (4). Vibrating conveyor belts as a

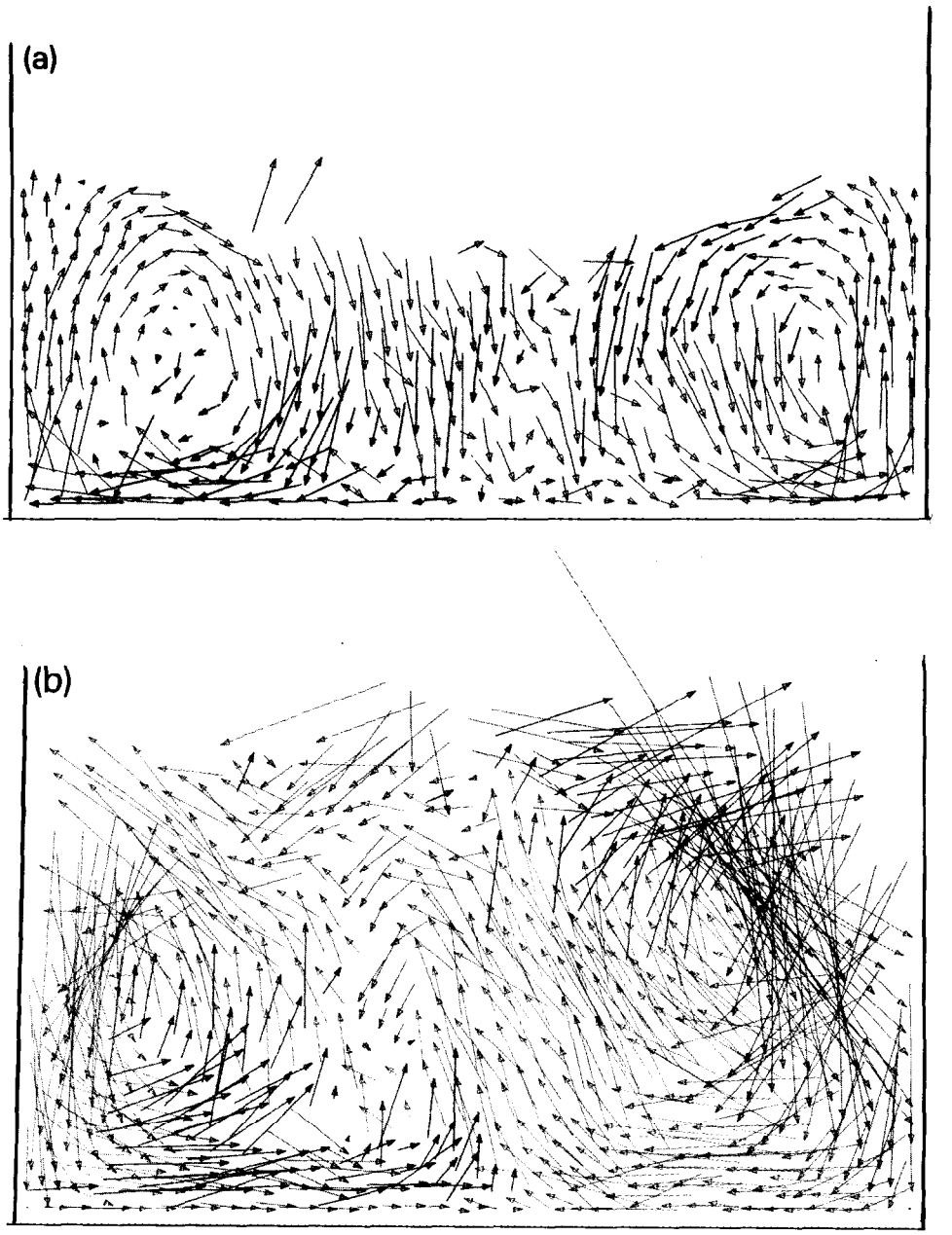

Fig. 3. Displacements after 10 cycles in a system with fixed vertical walls for $B = 0$, $w = 0.5$, $Y = 5000/d_0$, $f = 20$ Hz, averaged over 10 cycles. (a) $\gamma = 80g$, $N = 400$, $L = 40d_0$, $A_0 = 3.0d_0$, $\gamma_s = 0$; (b) $N = 600$, $L = 44d_0$, $A_0 = 1.25d_0$, $\gamma_s = 100g$. The colours code the quadrant into which the particles move (green: left-up, blue: left-down, in (a) purple in (b) orange: right-down, red: right-up).

means of transportation are very typical for granular media, since neither solids nor fluids can be moved on them and are used for instance in the pharmaceutical industry to transport pills [31].

We measured density and velocity profiles as a function of height z in the steady state. Close to the belt the local density is very small, then it has a maximum and at large heights it falls off. Only at low frequency the local density shows a plateau extending up to larger z values. When the frequency increases, the maximum of the local density decreases and the density profile smears out. The tail at large heights indicates the existence of particles in a gas-like state above the free surface of the packing. The density profile is rather independent of the angle of vibrations, which means that the vertical component of the vibration determines almost completely the vertical density of the beads. When the friction coefficients decrease, the system becomes more gas-like. Only very close to the belt the profiles seem independent of the friction. The velocity profiles exhibit a well-developed plateau, showing that almost all particles move at the same speed. Obviously, the velocity increases with increasing frequency and decreasing angle of vibrations and for $\gamma_s = 0$ the velocity is zero. For $\gamma_s \geq 50g$ the velocity profile depends only very weakly on the shear friction coefficient.

Let us consider the trajectories of the particles during one cycle of shaking. When the frequency is low enough all the beads move synchronously along elliptic trajectories. The tilting angle of these ellipses increases with the angle of vibrations. For smaller shear friction coefficients γ_s the tilting angle tends to $\pi/2$, provided the vibration frequency is low enough. When the beads start to flow, the character of their trajectories changes: at not too high frequencies they move along sinusoidal curves as shown in fig. 4a. With increasing frequency, the trajectories become flatter and at the highest frequencies we observe a nearly horizontal flow (see fig. 4b). A decrease of the vibration angle makes the horizontal motion more pronounced. A similar effect occurs when the friction coefficients are increased. For vanishing shear friction γ_s the beads move essentially vertically.

Next we checked how a circular obstacle inserted into the system influences the flow. To this end, a fixed circular body was inserted at $x_1 = L/2$, $z_1 = A_z$. The diameter of the obstacle was varied from $d_1 = 0.1d_0$ to $d_1 = 2.5d_0$. The parameters characterizing the interactions of the obstacle with the particles were the same as in the case of particle–particle interactions. Note that due to the periodic boundary conditions, the obstacle is repeated along the belt. Even the presence of a rather small obstacle rapidly slows down the flow. In fig. 5 we see the trajectories of the particles for an obstacle of $d_1 = 1.5d_0$. Figs. 4 and 5 have the same parameters so that without the obstacle fig. 5a would look like fig. 4a and fig. 5b like fig. 4b. Clearly the presence of the obstacle changes the

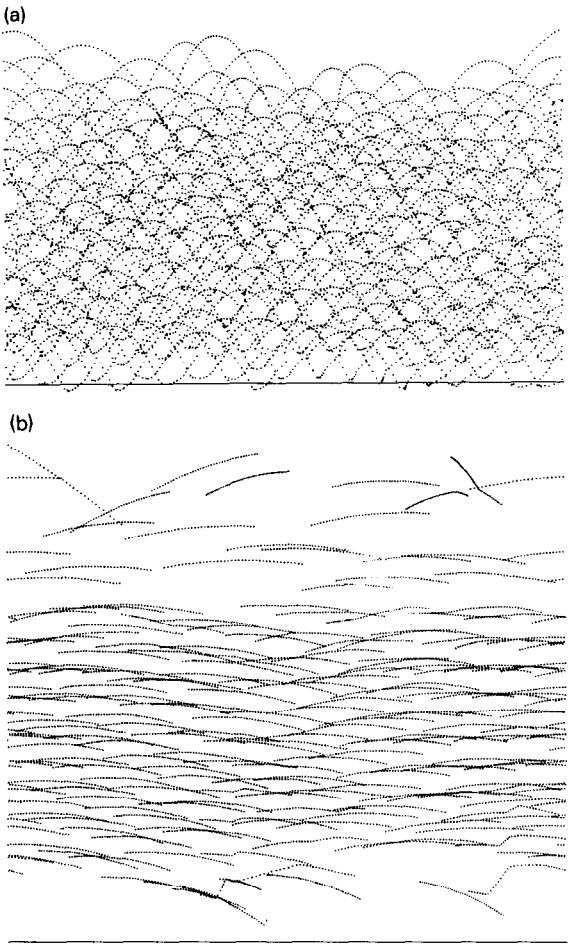

Fig. 4. Trajectories of the particles in steady state during a single cycle. The position of each particle is plotted after every 50 time-steps. The plots were obtained for $A_z = d_0$, $\alpha = \pi/4$, $\gamma = \gamma_s = 50g$, and (a) $f = 20$ Hz and (b) $f = 80$ Hz.

trajectories of all the particles considerably. So, we cannot treat the obstacle as only locally influencing the flow, because the stiff repulsion between particles generates long-range correlations.

Using similar techniques but including the Coulomb (dynamic) friction and rotations of particles as in ref. [5] new simulations were made recently for the flow out of a hopper [25], flow down an inclined chute [28] and flow through a pipe [32]. Because of the lack of static friction the simulations of the hopper have not reproduced the observed density waves [9] but nevertheless they find the existence of a minimal outlet diameter due to some kind of arching which is larger for equal sized particles than for randomly distributed radia. The

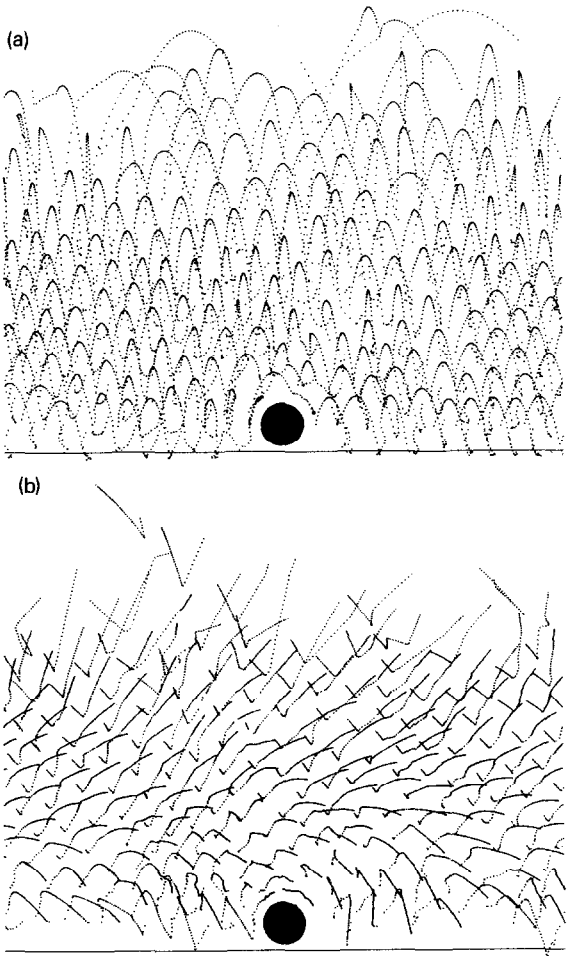

Fig. 5. Trajectories of the particles flowing in the presence of an obstacle for $A_z = d_0$, $\alpha = \pi/4$, $\gamma = \gamma_s = 50g$. In (a) the frequency was 20 Hz, whereas in (b) 80 Hz. The obstacle of diameter $d_1/d_0 = 1.5$ is given by the full circle.

simulations down an inclined plane very accurately reproduce the various types of flow and the dependence of the velocity profile on the smoothness of the plane as they were observed in recent experiments [33]. Flow through a vertical pipe with rough walls [32] was found to generate density waves. Their appearance and speed strongly depends on small details of the initial positions of the grains. The similarity to the experimental situation was illustrated in a movie. Including also the static friction into the simulation as in ref. [29], heaps and avalanches were obtained and various characteristic angles (repose, minimal stability, tilting) were measured [30].

Subjected to an external force granular materials locally perform rather statistical motions due to the random nature of the size and shape of grains and their contacts. For example, on the loudspeaker the individual grains chaotically jump up and down forming a gas-like cloud of colliding particles. Also inside a shear-cell [12,27,34] or flowing down an inclined chute [13,28,33] in addition to a laminar flow with a well-defined (average) velocity profile, one has Brownian-like motion of the particles perpendicular to the flow direction.

The above observations have inspired several authors to use thermodynamic concepts to describe granular media. On one hand a "granular temperature" T_{gr} has been defined [1,27,35,36] as $T_{gr} = \langle \boldsymbol{v}^2 \rangle - \langle \boldsymbol{v} \rangle^2$, i.e. proportional to the kinetic energy surplus with respect to the global motion. This definition is only thermodynamically justified if an equipartition theorem exists which is not the case for granular particles since they dissipate energy at collisions. On the other hand, Edwards and collaborators [37] have put forward another idea: Based on the important observation that granular materials do not conserve energy they proposed to consider the volume V to replace the internal energy in the usual thermodynamic formalism and define a temperature-like quantity $X = \partial V / \partial S$ which they called "compactivity". Although formally intact, this formalism is not easy to justify since in many real situations like on the vibrating table or on an inclined plane, the volume is not well limited at large heights. While Edward's approach seems intuitively correct for dense packings and the definition of T_{gr} reasonable in the limit of strong internal motions or weak dissipation, they fail in the corresponding opposite limit.

Let us present in the following a thermodynamic approach to granular materials [38] founded on similar principles as equilibrium thermodynamics which incorporates at least partially the intuitive pictures of previous work: We shall consider subsystems sufficiently small to have no velocity or density gradients and for which the energy flux into them is such that energy dissipation is homogeneous. Energy conservation implies that $\Delta I = \Delta E_{int} + \Delta D$ where ΔD is the energy dissipated in a given time and ΔI is the energy that was pumped into the system while ΔD was dissipated in order to maintain a steady state. The internal energy E_{int} is like in traditional thermodynamics the kinetic and potential energy of all the degrees of freedom of the grains as elastic bodies (translation, rotation, elasticity, etc.). One can now treat the excess dissipated energy ($\Delta \mathcal{D} = \Delta D - \Delta I$) in a similar way as the heat in usual thermodynamics. Since the dissipated energy is proportional to the sum of normal forces f_n^i that push the particles together during collision i one can express changes in $\mathcal{D}$ as $\delta \mathcal{D} = \wp \delta C$ where $\wp$ is an internal pressure acting at collisions that we empirically define as $\wp = \rho \langle f_n^i / A_i \rangle$ where A_i is the area of contact of collision i and the average is performed over all collisions. We define the density ρ of collisions as the number of collisions per unit volume and unit

time. The extensive quantity C has a geometrical interpretation and plays the role of a potential. It should in fact be proportional [38] to the overlap volume V_{0v} that one has for technical reasons in MD simulations, which can be defined more precisely as the sterically excluded volume that would arise if the centers of mass of the particles follow the real trajectories but one does not take into account the elasto-plastic deformation. The "equilibrium" – which is in fact a steady state driven by the energy flux – can be defined as the ensemble *minimizing* C and one can *postulate* in analogy to the second law of thermodynamics that C should decrease for any change of state at constant internal energy E_{int}: $\Delta C \leqslant 0$. Physically such a behaviour seems naturally be driven by the elastic repulsion between colliding (overlapping) grains.

As in usual thermodynamics one can now work in different ensembles. Naturally one would work at fixed $\wp$ (granular ensemble) in which a granular potential G_r can be defined as $G_r = E_{\text{int}} + \wp C$ and where at constant $\wp$ the equilibrium is given by the minimum of G_r. The response function κ defined as $\kappa = \partial \mathcal{D} / \partial \wp = \wp \, \partial C / \partial \wp$ measures how much more energy can be dissipated if $\wp$ is increased. It should characterize the "fluidization" transition and from its frequency dependence one might identify $1/f$ noise [10]. On top of the granular ensemble one can build up the traditional body of thermodynamics as if the grains were a gas of particles interacting elastically. One can fix or free the number N of particles, define a "granular" temperature T_g and entropy S or impose to the system either an external volume V or an external pressure p. A novelty for granular media is that one could also impose an external shear τ or its conjugate, the dilatancy V_d [11,12].

By considering a "state" to be given by the positions, orientations, linear and angular velocities of the grains as rigid bodies, the entropy is well defined as noted already in ref. [18]. A reasonable definition for a "granular" temperature T_g would then be: $T_g = (\partial G_r / \partial S)_\wp$ which is, in fact, similar to the one defined previously [1,27,35,36]. Experimentally $\wp$ and T_g are independent control parameters of the system: T_g is essentially driven by the amount ΔI of energy that is fed into the system per unit time. $\wp / T_g$ depends mainly on the density of collisions and can therefore increase by fragmenting the grains into smaller pieces. (Note that when a given grain is split into eight pieces, the cross section of each individual piece decreases by a factor four, so that $\wp$ will increase by two.)

We have described within a thermodynamic formalism the fluctuations arising from the constant flux and dissipation of energy that drives a granular material's kinematic behaviour. By separating the dissipative degree's of freedom (friction and plasticity) from the conservative ones (translation, rotation, elasticity) we define a "granular ensemble" coupled to a "dissipate bath", which is in fact the one in which experimental and numerical measure-

ments are usually performed. We introduce a potential C which physically is the contact volume of the collisions. It would be interesting to give also a statistical interpretation to C in order to define it as a "dissipative potential" [39]. The fluctuating internal energy is replaced by a granular potential G_r controlled by an intensive variable $\wp$, conjugate to C. We proposed in ref. [38] various numerical tests for the assumptions that we have made in this theory.

With a rather simple two-dimensional description of a granular medium as an ensemble of inelastic spherical particles with shear friction we have shown that many interesting rheological properties can be reproduced. Various types of convection can occur on a vibrating plate and density waves appear during the flow through a pipe. It is not straightforward to determine the material constants corresponding to some parameters of the model, like γ and γ_s, and so a quantitative comparison with experiments in most cases involves some fit parameters. More realistic models including real static and dynamic friction, rotations of particles, variations in the particle shapes, etc., increase the number of parameters but are needed to establish a closer contact to reality. Three-dimensional simulations must also be performed since many phenomena seem to be due to steric effects.

I thank my collaborators J.A.C. Gallas and S. Sokolowski for their patience and J. Lee, C. Moukarzel, T. Pöschel and G. Ristow for many enlightening discussions.

References

[1] H.M. Jaeger and S.R. Nagel, Science 255 (1992) 1523.
[2] S.B. Savage, in: Disorder and Granular Media, D. Bideau, ed. (North-Holland, Amsterdam, 1992); S.B. Savage, Adv. Appl. Mech. 24 (1984) 289; C.S. Campbell, Annu. Rev. Fluid Mech. 22 (1990) 57.
[3] J.C. Williams, Powder Techn. 15 (1976) 245.
[4] A. Rosato, K.J. Strandburg, F. Prinz and R.H. Swendsen, Phys. Rev. Lett. 58 (1987) 1038; Powder Techn. 49 (1986) 59; P. Devillard, J. Phys. (Paris) 51 (1990) 369.
[5] P.K. Haff and B.T. Werner, Powder Techn. 48 (1986) 239.
[6] M. Faraday, Philos. Trans. R. Soc. London 52 (1831) 299.
[7] P. Evesque and J. Rajchenbach, Phys. Rev. Lett. 62 (1989) 44; C.R. Acad. Sci. Ser. 2, 307 (1988) 1, 223; C. Laroche, S. Douady and S. Fauve, J. Phys. 50 (1989) 699; P. Evesque, J. Phys. (Paris) 51 (1990) 697; J. Rajchenbach, Europhys. Lett. 16 (1991) 149.
[8] J. Walker, Sci. Am. 247 (1982) 167; F. Dinkelacker, A. Hübler and E. Lüscher, Biol. Cybern. 56 (1987) 51.
[9] G.W. Baxter, R.P. Behringer, T. Fagert and G.A. Johnson, Phys. Rev. Lett. 62 (1989) 2825.
[10] C.-h. Lui and S.R. Jaeger, Phys. Rev. Lett. 68 (1992) 2301; G.W. Baxter, PhD thesis.
[11] O. Reynolds, Philos. Mag. S. 20 (1885) 469.
[12] Y.M. Bashir and J.D. Goddard, J. Rheol. 35 (1991) 849.

[13] S.B. Savage, J. Fluid Mech. 92 (1979) 53; G.M. Homsy, R. Jackson and J.R. Grace, J. Fluid Mech. 236 (1992) 477; S.B. Savage and K. Hutter, J. Fluid Mech. 199 (1989) 177.
[14] G.W. Baxter and R.P. Behringer, Phys. Rev. A 42 (1990) 1017; Physica D 51 (1991) 465.
[15] H. Caram and D.C. Hong, Phys. Rev. Lett. 67 (1991) 828.
[16] J.A.C. Gallas, H.J. Herrmann and S. Sokołowski, Physica A 189 (1992) 437.
[17] E. Clement and J. Rajchenbach, Europhys. Lett. 16 (1991) 133.
[18] P. Evesque, E. Szmatula and J.-P. Denis, Europhys. Lett. 12 (1990) 623; O. Zik and Stavans, Europhys. Lett. 16 (1991) 255; O. Zik, J. Stavans and Y. Rabin, Europhys. Lett. 17 (1992) 315.
[19] G. Rátkai, Powder Techn. 15 (1976) 187.
[20] J.A.C. Gallas, H.J. Herrmann and S. Sokołowski, Phys. Rev. Lett. 69 (1992) 1371.
[21] Y-h.Tagushi, Phys. Rev. Lett. 69 (1992) 1367.
[22] J.A.C. Gallas, H.J. Herrmann and S. Sokołowski, J. Phys. (Paris) II 2 (1992) 1389.
[23] M.P. Allen and D.J. Tildesley, Computer Simulation of Liquids (Oxford Univ. Press, Oxford, 1987).
[24] D. Tildesley, in: Computational Physics, R.D. Kenway and G.S. Pawley, eds., NATO Advanced Study Institute (Edinburgh Univ. Press, Edinburgh, 1987).
[25] G. Ristow, J. Phys. (Paris) I 2 (1992) 649.
[26] D.C. Hong and J.A. McLennan, Physica A 187 (1992) 159.
[27] C.S. Campbell and C.E. Brennen, J. Fluid Mech. 151 (1985) 167; P.A. Thompson and G.S. Grest, Phys. Rev. Lett. 67 (1991) 1751; D.M. Hanes and D.L. Inman, J. Fluid Mech. 150 (1985) 357; O.R. Walton and R.L. Braun, J. Rheol. 30 (1986) 949.
[28] T. Pöschel, preprint HLRZ 22/92.
[29] P.A. Cundall and O.D.L. Strack, Géotechnique 29 (1979) 47.
[30] J. Lee and H.J. Herrmann, preprint HLRZ 44/92.
[31] H. Schmidt and I. Peschl, Fördern Heben 15 (1965) 606.
[32] T. Pöschel, preprint HLRZ 67/92.
[33] T.G. Drake, J. Geophys. Res. 95 (1990) 8681.
[34] R.A. Bagnold, Proc. R. Soc. London A 295 (1966) 219; H.M. Jaeger, C.-h. Liu, S.R. Nagel and T.A. Witten, Europhys. Lett. 11 (1990) 619.
[35] S. Ogawa, Proc. US–Japan Symp. on Continuum Mechanics and Statistical Approaches to the Mechanics of Granular Media, S.C. Cowin and M. Satake, eds. (Gakujutsu Bunken Fukyu-kai, 1978) p. 208.
[36] J.T. Jenkins and S.B. Savage, J. Fluid Mech. 130 (1983) 186; H.M. Jaeger, C.-h. Lui and S.R. Nagel, Phys. Rev. Lett. 62 (1989) 40.
[37] S.F. Edwards and R.B.S. Oakeshott, Physica A 157 (1989) 1080; S.F. Edwards, J. Stat. Phys. 62 (1991) 889; A. Mehta and S.F. Edwards, Physica A 157 (1989) 1091.
[38] H.J. Herrmann, preprint HLRZ 43/92.
[39] I. Prigogine, Bull. Acad. R. Belg. Cl. Sci. 31 (1954) 600; P. Glansdorff and I. Prigogine, Thermodynamic Theory of Structure, Stability and Fluctuations (Wiley–Interscience, New York, 1971); Lord Rayleigh, Proc. Lond. Math. Soc. 4 (1873) 357.